

## Dynamics of Ostwald ripening in the presence of surfactants

Jian Hua Yao and Mohamed Laradji

*Centre for the Physics of Materials, Department of Physics, Rutherford Building, McGill University,  
3600 rue University, Montréal, Québec, Canada H3A 2T8*

(Received 13 February 1992; revised manuscript received 31 August 1992)

We show that the effect of surfactants on Ostwald ripening can be reduced to the problem of Ostwald ripening with a time-dependent surface tension. Since the latter can be mapped onto a constant-surface-tension case with a nonlinear time transformation, we can systematically study the effect of surfactants without much difficulty. As a result, we find that the scaled distribution function of droplet size remains the same, but the average domain size no longer obeys the power-law growth  $t^{1/3}$ . Furthermore, we show that the average domain size and the total number of droplets saturate at very late times. The former is inversely proportional to the surfactant density at the interfaces, while the latter is proportional to the square (cube) of the surfactant density at the interfaces in two dimensions (three dimensions). We also find that different growths for different surfactant densities at the interface can be written in a crossover scaling form. These results qualitatively confirm the recent results of Laradji *et al.* [J. Phys. A **44**, L629 (1991)].

PACS number(s): 82.70.Kj, 64.60.My

### I. INTRODUCTION

When a binary mixture is quenched from the disordered phase into the two-phase metastable region (where the volume fraction of the minority component is quite small), the minority component condenses into small spherical droplets. The average droplet radius  $\bar{R}(t)$  grows with time, but the total number of the droplets decreases with time due to the fact that the system tries to reduce its total interfacial free energy. This phenomenon is known as Ostwald ripening. In the limit of zero volume fraction of the minority phase, Lifshitz and Slyozov [1, 2] obtained the following results: the average domain size grows as  $\bar{R} = (Kt)^{1/3}$  and the distribution function of droplet sizes obeys the scaling form  $f(R, t) \propto F(R/\bar{R})/\bar{R}^4$  at late times, where  $K$  is the dimensionless coarsening rate. These two features, power-law growth and scaling, are considered to be generic in the kinetics of first-order phase transitions [3].

Extensions of the theory of Lifshitz and Slyozov to nonzero volume fractions and two-dimensional systems, using both analytical and numerical methods, have been proposed by many groups [4–10]. A larger coarsening rate and a broad distribution function have been obtained for nonzero volume fractions. Furthermore, Yao *et al.* [11] recently developed a nonlinear approach to Ostwald ripening, which treats both two and three dimensions in the same manner. The two- and three-dimensional results of this approach are in agreement with numerical simulations and experiments [11].

The goal of the present paper is to apply that Ostwald ripening theory [11] to systems which consist of two immiscible components and surfactants. When surfactants are mixed with two immiscible components, such as water and oil, the dynamics are different from that of a pure binary mixture due to the fact that the head of

a surfactant interacts attractively with one component, while its tail interacts attractively with the second component. As a result, surfactants preferably adsorb at the interfaces. During coarsening, the total interfacial area decreases; therefore, the concentration of surfactants at the interfaces increases, leading to a decrease of the surface tension between the segregating domains.

Consequently, the effects of surfactants can be reduced to that of a time-dependent surface tension. However, for different values of constant surface tension, growth follows with scaling and a  $t^{1/3}$  growth law, but the prefactor  $K$  changes. Thus for a time-dependent surface tension (where its time variation is sufficiently slow so that interfaces are always well defined), we anticipate that the growth law should change due to the induced time dependence of  $K$ , but that the scaling function should not. Furthermore, all that is required to map the time-dependent surface tension Ostwald ripening problem onto the constant surface tension one is the appropriate time transformation. This is what we shall show below, where we give explicit forms for  $\bar{R}(t)$  and  $f(R, t)$ .

Both theoretical and experimental work have shown that ternary mixtures containing surfactants undergo microphase separation into small segregated domains of two immiscible components, stabilized by surfactant films such as in emulsions, microemulsions, colloids, and foams [12–18]. Typical surfactants are amphiphilic molecules. Because these molecules have hydrophilic heads and hydrophobic tails, they produce emulsions or microemulsions when mixed with water and oil, and they can also produce foams when mixed with water and air.  $A$ - $B$  diblock copolymers also behave like surfactants when mixed with a blend of  $A$  and  $B$  homopolymers, and produce stable emulsions [19, 20].

Recently, Laradji *et al.* [21] have studied these dynamics by means of a time-dependent Ginzburg-Landau

model for equal volume fractions of the two immiscible components and found a slow and nonalgebraic growth for nonzero volume fractions of surfactants. Moreover, they found that the growth becomes even slower for higher surfactant volume fractions. The domain growth saturated at late times to a value inversely proportional to the surfactant volume fraction [21]. These results are qualitatively confirmed by Kawakatsu and Kawasaki using a “hybrid model” [22].

The organization of this paper is as follows. In Sec. II, we briefly summarize the theory of Ostwald ripening [11] and present our modified equations for the case in which surfactants are present. In Sec. III, we present the general solutions for systems with a time-dependent surface tension, and then focus on surfactant systems. We close this article with a short conclusion in Sec. IV.

## II. BASIC EQUATIONS

The fundamental equation is the many-particle diffusion equation in the quasistationary approximation describing Ostwald ripening [11],

$$\mathcal{D}\nabla^2\Theta(\mathbf{r}) = a \sum_{i=1}^N B_i \delta(\mathbf{r} - \mathbf{r}_i), \quad (1)$$

where  $a = 2\pi^{D/2}/\Gamma(D/2)$ ,  $D$  is the spatial dimension,  $\Theta(\mathbf{r}) = [C(\mathbf{r}) - C_\infty]/C_\infty$ ,  $C(\mathbf{r})$  is the local concentration field of the minority component outside the droplets, and  $C_\infty$  is the equilibrium concentration at a flat interface.  $N$  is the number of droplets in the system,  $\mathcal{D}$  is the diffusion coefficient,  $\mathbf{r}_i$  gives the location of the  $i$ th droplet, and  $B_i$  gives the strength of the source of diffusion current. This is the multiparticle diffusion equation in the quasistationary approximation, where  $\partial\Theta/\partial t$  is neglected because the concentration changes very slowly at late times. The  $\delta$  functions on the right-hand side of Eq. (1) result from the assumption that droplet locations remain fixed in space and the distances between droplets are much larger than the average droplet size. This is a very good description for systems with small volume fractions.  $\Theta(\mathbf{r})$  satisfies the Gibbs-Thomson boundary condition at the curved surface of each droplet:

$$\Theta(\mathbf{r})|_{|\mathbf{r}-\mathbf{r}_i|=R_i} = \mu/R_i, \quad i = 1, \dots, N; \quad (2)$$

$\lim_{r \rightarrow \infty} \Theta(\mathbf{r}) = \Theta_{av}$ , where  $\Theta_{av}$  is the average concentration outside the droplets, and  $\mu = (D-1)\gamma_0 V_m/RT$ .  $\gamma_0$ ,  $R_g$ ,  $T$ , and  $V_m$  represent the surface tension, the gas constant, the temperature, and the molar volume in  $D = 3$  (molar area in  $D = 2$ ), respectively. Here we consider a conserved system in which the volume fractions of the two separating components are conserved during the phase separation process. Consequently, the conservation law obeys

$$\sum_{i=1}^N B_i = 0, \quad (3)$$

and the growth law is given by

$$\frac{dR_i}{dt} = \frac{B_i}{R_i^{D-1}}. \quad (4)$$

Since Eq. (3) resembles charge neutrality and Eq. (1) is analogous to the Coulomb interaction in an electron gas, a Thomas-Fermi-type approximation can reduce Eq. (1) to a one-body problem [11]:

$$\nabla^2\Theta - \xi^{-2}\Theta + \xi^{-2}\Theta_{av} = aB_i\delta(\mathbf{r} - \mathbf{r}_i) \quad (5)$$

in the vicinity of the  $i$ th droplet, where the screening length  $\xi$  is given by

$$\xi^{-2} = \frac{a}{V'} \int_0^\infty \frac{f(R, t)}{V(R/\xi, R)} dR. \quad (6)$$

Here  $V'$  is the system volume, and  $V(R/\xi, R)$  is the Green's function of Eq. (5). In  $D = 3$ ,  $V(R/\xi, R) = \exp(-R/\xi)/R$ ; in  $D = 2$ ,  $V(R/\xi, R) = K_0(R/\xi)$ , where  $K_0$  is the zeroth-order modified Bessel function. Applying the solution of Eq. (5) at the boundaries of droplets gives us

$$\mu/R_i = \Theta_{av} - B_i V(R_i/\xi, R_i) \quad (7)$$

for  $i = 1, \dots, N$ . By substituting the solution  $B_i$  and  $\Theta_{av}$  of Eqs. (3) and (7) into Eq. (4), we obtain

$$\frac{dR}{dt} = \frac{\mathcal{D}\mu R^{1-D}}{V(R/\xi, R)} \left\{ \frac{[\overline{RV(R/\xi, R)}]^{-1}}{[V(R/\xi, R)]^{-1}} - \frac{1}{R} \right\}, \quad (8)$$

where the bar is defined as

$$\overline{A} \equiv \frac{\int_0^\infty A f(R, t) dR}{\int_0^\infty f(R, t) dR}. \quad (9)$$

Furthermore, the continuity equation is given by

$$\frac{\partial f(R, t)}{\partial t} + \frac{\partial}{\partial R}[\dot{R}f(R, t)] = 0, \quad (10)$$

and the conservation law Eq. (3) can be rewritten as

$$\frac{v}{V'} \int_0^\infty R^D f(R, t) dR = \phi, \quad (11)$$

where  $v = \pi^{D/2}/\Gamma(D/2 + 1)$ , and  $\phi$  is the volume (area in  $D = 2$ ) fraction of the droplets. Equations (6), (8), (10), and (11) are the basic equations describing Ostwald ripening in the absence of surfactants.

We now consider the effects of surfactants on the dynamics of Ostwald ripening. During the coarsening, the total area of the interface (total length of the interface for  $D = 2$ ) decreases with time as  $a \int_0^\infty R^{D-1} f(R, t) dR$ . At late times, the local density of surfactants inside the droplets or in the bulk reaches a steady-state value that is usually very small. However, surfactants can diffuse from the interfaces of the shrinking droplets to those of the growing ones in a similar manner as the minority component does without changing its concentration in the bulk. In fact, this is a quasistationary approximation. As a result, the total number of surfactants at the interfaces is conserved, and the interfacial density of surfactants in-

creases with time. A higher density of surfactants at the interface corresponds to a reduced surface tension due to the screening effect of surfactants at the boundaries. These effects have been observed in a previous numerical study [21]. With the simplest assumption that surfactants uniformly distribute at the interfaces, the surface tension should decrease proportionally to the interfacial density of surfactants, i.e.,  $\gamma(t) = \gamma_0 \epsilon(t)$  and

$$\epsilon(t) = 1 - \frac{\alpha'}{\int_0^\infty R^{D-1} f(R, t) dR}, \quad (12)$$

where  $\alpha'$  is a surfactant screening coefficient proportional to the total number of surfactants at the interface. Replacing  $\gamma_0$  by  $\gamma(t)$ , we obtain

$$\frac{dR}{dt} = \frac{\epsilon(t) R^{1-D}}{V(R/\xi, R)} \left\{ \frac{[RV(R/\xi, R)]^{-1}}{[V(R/\xi, R)]^{-1}} - \frac{1}{R} \right\}, \quad (13)$$

where we have made the following transformations:  $R' = R/\mu$ ,  $t' = tDC_\infty/\mu^2$ ,  $\xi = \xi'/\mu$ , and  $f'(R, t) = \mu^3 f(R, t)$ , and then  $R'$ ,  $t'$ ,  $\xi'$ , and  $f'(R, t)$  were replaced by  $R$ ,  $t$ ,  $\xi$ , and  $f(R, t)$ , respectively.

The problem of Ostwald ripening with a time-dependent surface tension can be straightforwardly mapped onto the usual constant surface tension problem by introducing the following nonlinear time transformation

$$\tau = \int_0^t \epsilon(t') dt'. \quad (14)$$

This transformation leads us to rewrite Eqs. (10) and (13) as follows:

$$\frac{\partial f(R, \tau)}{\partial \tau} + \frac{\partial}{\partial R} [\dot{R} f(R, \tau)] = 0 \quad (15)$$

and

$$\frac{dR}{d\tau} = \frac{R^{1-D}}{V(R/\xi, R)} \left\{ \frac{[RV(R/\xi, R)]^{-1}}{[V(R/\xi, R)]^{-1}} - \frac{1}{R} \right\}, \quad (16)$$

where now  $\dot{R} = dR/d\tau$ .

These equations are of exactly the same form as the Ostwald ripening problem with a constant surface tension with a new time variable  $\tau$  [11]. Thus we can now “read off” the results for  $\bar{R}(t)$  and  $f(R, t)$  via the transformation  $\tau = \tau(t)$ . We speculate that this is generally true, although we have shown it here only within our mean-field approximation.

### III. SOLUTIONS AND DISCUSSION

In this section, we present the solution of our equations for the case of an arbitrary time-dependent surface tension and then treat the effects of surfactants as a special case. For  $\phi \leq 0.06$  in  $D = 3$  or  $\phi \leq 0.085$  in  $D = 2$ , Eqs. (6), (11), (15), and (16) have the following scaling solution [11]:

$$f(R, \tau) \propto \frac{g(z)}{u^{D+1}(\tau)} \quad (17)$$

so long as  $\epsilon(t)$  does not depend on individual droplet radius  $R$ , where  $z = R/u(\tau)$ . Here  $g(z)$  is a scaled, normalized droplet distribution function satisfying

$$g(z) = \begin{cases} \frac{-\lambda D}{w(z, \lambda)} \exp\left(\lambda D \int_0^z w^{-1}(z', \lambda) dz'\right) & \text{if } 0 < z < z_0 \\ 0 & \text{otherwise,} \end{cases} \quad (18)$$

where

$$w(z, \lambda) = z^{1-D}(\sigma - z^{-1})/V(z/\eta, z) - \lambda z,$$

$$\sigma = \int_0^\infty \frac{g(z)}{zV(z/\eta, z)} dz / \int_0^\infty \frac{g(z)}{V(z/\eta, z)} dz,$$

$$\eta^{-2} = \frac{\phi D}{\int_0^\infty z^D g(z) dz} \int_0^\infty \frac{g(z)}{V(z/\eta, z)} dz,$$

$$w(z_0, \lambda) = 0, \quad \left. \frac{dw(z, \lambda)}{dz} \right|_{z=z_0} = 0,$$

and  $u(\tau)$  obeys

$$u^3(\tau) - u^3(0) = 3\lambda\tau. \quad (19)$$

From the definition Eq. (9), the average droplet radius then follows

$$\bar{R}^3(\tau) - \bar{R}^3(0) = K(\phi)\tau, \quad (20)$$

where  $K(\phi) = 3\lambda z_{\text{av}}^3$  [23], and  $z_{\text{av}} = \int z g(z) dz$  [11]. Equation (18) indicates that the scaled distribution function is entirely independent of the surface tension  $\epsilon(t)$ , while Eq. (20) shows that for any time-dependent surface tension, the average droplet radius grows in the same manner in the new time frame  $\tau$ . This solution is of course acceptable as long as  $\bar{R}$  is much larger than the small length scales in the system.

In general, if  $\lim_{t \rightarrow \infty} \tau/t = \infty$ , the growth is faster than  $t^{1/3}$ . On the other hand, if  $\lim_{t \rightarrow \infty} \tau/t = 0$  but  $\lim_{t \rightarrow \infty} \tau = \infty$ , the growth is slower than  $t^{1/3}$ , but the system undergoes a complete phase separation even if the surface tension vanishes; i.e., if  $\lim_{t \rightarrow \infty} \epsilon(t) = 0$ . In contrast, if  $\lim_{t \rightarrow \infty} \tau$  converges,  $\tau$  does not approach infinity even if  $t$  does. In this case, the system experiences an incomplete (or micro-) phase separation. These are the general features of Ostwald ripening with a time-dependent surface tension.

In order to describe quantitatively the effects of the time dependence of the surface tension, we now focus on concrete forms of  $\epsilon(t)$ . We, first of all, study a simple case in which  $\epsilon(t)$  decreases from one constant to another one:  $\epsilon(t) = 1 - \delta \tanh[(t - t_0)/\tau']$ . In this case,  $\tau$  follows

$$\tau = t - \delta\tau' \ln \left[ \cosh\left(\frac{t - t_0}{\tau'}\right) / \cosh\left(\frac{t_0}{\tau'}\right) \right]. \quad (21)$$

In the limit  $\tau' \rightarrow 0$ , i.e., the surface tension changes abruptly from  $1 + \delta$  to  $1 - \delta$  at  $t = t_0$ , the above equation reduces to

$$\tau = t[1 - \delta \operatorname{sgn}(t - t_0)] . \quad (22)$$

In this case, the growth crosses over from  $[K(\phi)(1 + \delta)t]^{1/3}$  to  $[K(\phi)(1 - \delta)t]^{1/3}$ , as demonstrated in Fig. 1.

Another simple and interesting case is where  $\epsilon(t)$  decreases (or increases) in time as  $\epsilon(t) = [(t + t_0)/\tau']^{-\nu}$ . After integrating Eq. (14), we obtain

$$\tau = \begin{cases} \tau' \ln(1 + t/t_0) & \text{if } \nu = 1 \\ \frac{\tau'}{1 - \nu} \left(\frac{t_0}{\tau'}\right)^{1-\nu} [(1 + t/t_0)^{1-\nu} - 1] & \text{otherwise} . \end{cases} \quad (23)$$

This result implies that the system undergoes a complete phase separation unless  $\nu > 1$ . The marginal case of  $\nu = 1$  shows clearly that even if the surface tension vanishes at  $t \rightarrow \infty$ , the system undergoes a complete but extremely slow phase separation. We can also consider the case where the surface tension decays exponentially, i.e.,  $\epsilon(t) = \exp(-t/\tau')$ .  $\tau$  then satisfies

$$\tau = \tau'[1 - \exp(-t/\tau')] . \quad (24)$$

In this case, the phase separation stops after a small  $\tau'$ . For the two cases studied above, the growth law is illustrated systematically in Fig. 2.

Finally, we study a more interesting and realistic problem: surfactant systems, in which  $\epsilon(t) = [1 - \beta u(t)]$ ,  $\beta = \alpha v \int_0^\infty z^D g(z) dz / \phi \int_0^\infty z^{D-1} g(z) dz$ , and  $\alpha = \alpha' / V'$  according to Eqs. (12) and (17). Thus  $u(t)$  satisfies the following implicit form:

$$\frac{1}{2\beta} [u^2(0) - u^2(t)] + \frac{1}{\beta^2} [u(0) - u(t)] + \frac{1}{\beta^3} \ln \frac{1 - \beta u(0)}{1 - \beta u(t)} = \lambda t , \quad (25)$$

and  $\bar{R}(t) = z_{\text{av}} u(t)$ . The average droplet radius is shown in Fig. 3 for different values of  $\beta$ , i.e., for different sur-

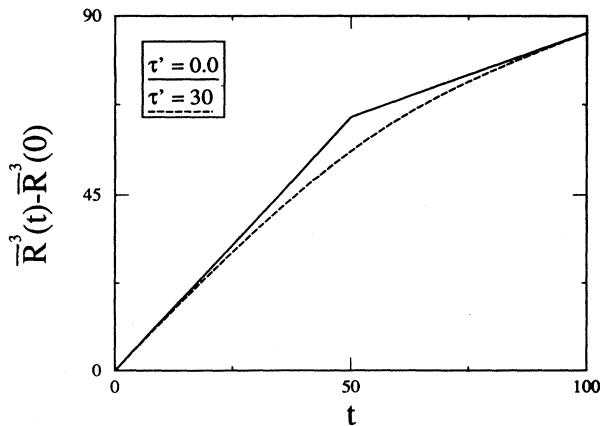


FIG. 1. Time evolution of Eq. (21): This figure demonstrates the prefactor of the average droplet radius crosses over from one constant to another. Here  $\delta = 0.5$ ,  $t_0 = 50$ ,  $\phi = 0.05$ , and  $K(0.05) = 0.856769$  (Ref. [11]).

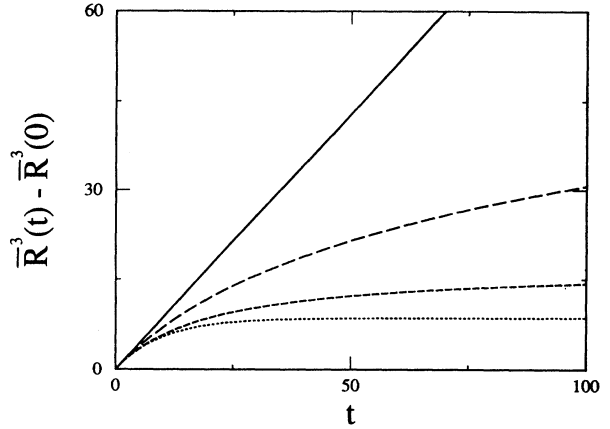


FIG. 2. Effects of the time dependence of the surface tension on the droplet growth. The solid line, long-dashed line, and dashed line present Eq. (23) for  $\nu = 0, 1$ , and  $2$ , respectively, where  $\tau' = 20$  and  $t_0 = 20$ ; the dotted line corresponds to Eq. (24) with  $\tau' = 10$ .  $\phi$  and  $K(\phi)$  are the same as in Fig. 1.

factant densities with  $\phi = 0.05$  in  $D = 3$ . This figure clearly shows that for a given  $\phi$ , as the surfactant screening coefficient  $\alpha$  increases, the coarsening procedure slows down, and the final average droplet size becomes smaller. Similarly, Fig. 4 shows, for a given surfactant screening coefficient  $\alpha$ , that as  $\phi$  decreases, the density of surfactants at the interfaces increases; therefore, the coarsening procedure slows down, and the final average droplet size becomes smaller as well [24]. Apparently, there are no essential differences between two and three dimensions.

It can be shown that at late times, the average radius of droplets can be written in the following crossover scaling form:

$$\bar{R}(t) = t^{1/3} h(\beta^3 t) \quad (26)$$

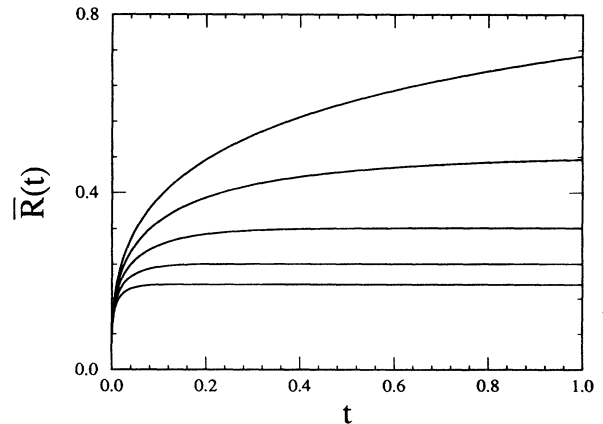


FIG. 3. Evolution of the average droplet radius  $\bar{R}(t)$  as a function of time  $t$  for the volume fraction  $\phi = 0.05$  in three dimensions [ $\bar{R}(t) = z_{\text{av}} u(t)$  and  $u(t)$  satisfies Eq. (25)]. Curves correspond to  $\beta = 1, 2, 3, 4$ , and  $5$  ( $\alpha = 2.2 \times 10^{-3}, 4.4 \times 10^{-3}, 6.6 \times 10^{-3}, 8.8 \times 10^{-3}$ , and  $1.1 \times 10^{-2}$  in  $D = 3$ ) from top to bottom, respectively.

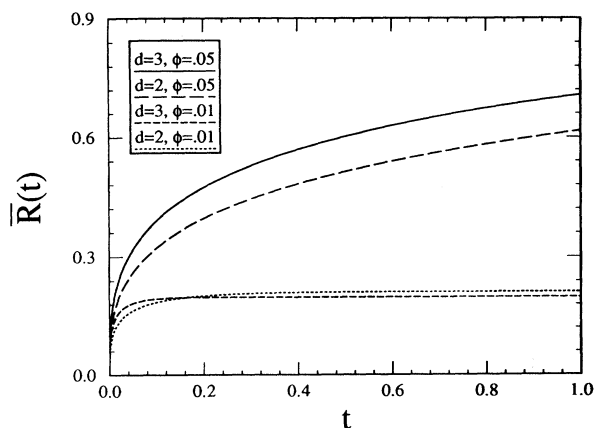


FIG. 4. Average droplet radius  $\bar{R}(t)$  evolving with time  $t$  for a fixed surfactant screening coefficient  $\alpha = 0.011$  in two dimensions, and  $\alpha = 0.014$  in three dimensions with volume fractions  $\phi = 0.01$  and  $0.05$ , where  $\bar{R}(t) = z_{av}u(t)$  and  $u(t)$  satisfies Eq. (25).

assuming  $u(0) \ll u(t)$ . In Fig. 5,  $h(x)$  is displayed as a function of  $x$  in  $D = 2$  and  $\phi = 0.05$ , essentially consistent with numerical simulations [21,25]. More explicitly, at late times  $u(t)$  actually satisfies

$$u(t) \simeq \frac{1}{\beta}(1 - e^{-\lambda\beta^3 t}), \quad (27)$$

where we have ignored  $u(0)$  and the first two terms in Eq. (25) due the fact that  $u(t) < 1/\beta$ , and  $u(0) \ll 1/\beta$ . Consequently,  $\bar{R}(t)$  and  $h(\beta^3 t)$  obey

$$\bar{R}(t) = \frac{z_{av}}{\beta}(1 - e^{-\lambda\beta^3 t}) \quad (28)$$

and

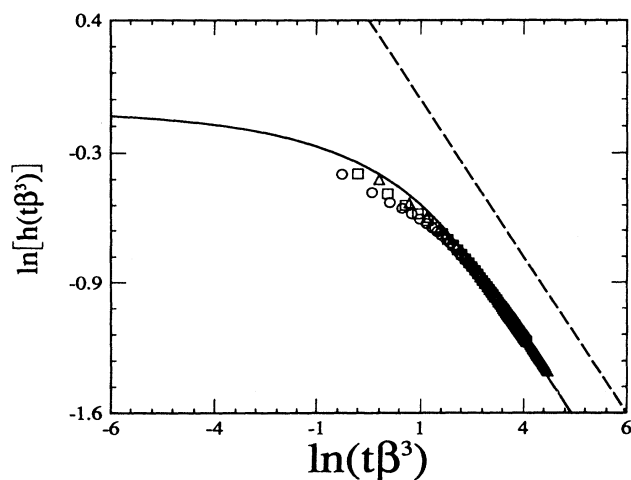


FIG. 5. Log-log plot of crossover scaling function  $h(\beta^3 t)$  vs  $\beta^3 t$ . The solid line is our two-dimensional result, Eq. (26), for  $\phi = 0.05$ . The symbols are the simulation results [21], where the different symbols correspond to different average surfactant densities. The dotted line has a slope of  $-\frac{1}{3}$ .

$$h(\beta^3 t) = \frac{z_{av}}{(\beta^3 t)^{1/3}}(1 - e^{-\lambda\beta^3 t}), \quad (29)$$

respectively. The shape of this crossover scaling function and its asymptotic behavior is quite similar to the one observed by Laradji *et al.* [21], though they studied the effects of surfactants on a phase separating bicontinuous system with  $\phi = 0.5$ , its largest possible value.

It is easy to see that when the screening effect of surfactants is negligible (i.e.,  $\alpha, \beta \rightarrow 0$ ), Eq. (25) reduces to  $u^3(t) - u^3(0) = 3\lambda t$  and becomes

$$\bar{R}^3(t) - \bar{R}^3(0) = K(\phi)t, \quad (30)$$

which is the usual growth law observed in Ostwald ripening as predicted by the novel Ostwald ripening theory [11]. To compare the differences between the dynamics of Ostwald ripening in the absence and in the presence of surfactants,  $\bar{R}^3(t) - \bar{R}^3(0)$  versus time is plotted in Fig. 6 for both cases. This figure shows clearly the drastic effects of surfactants on deviating the growth from simple power law. In fact, these effects can be easily understood by examining the time evolution of the surface tension Eq. (12), which asymptotically shows  $\epsilon(t) \sim \exp(-\beta^3 t)$ . Thus, as time approaches infinity,  $\epsilon(t)$  exponentially decays in time, and the growth practically stops after a few  $\beta^{-3}$  times as we have seen previously.

Another important quantity is the time evolution of the total number of droplets. According to the definition, at time  $t$ , this number obeys

$$N(t) = \int_0^\infty f(R, t) dR = \frac{N(0)\bar{R}^D(0)}{\bar{R}^D(t)}, \quad (31)$$

which is displayed in Fig. 7 as a function of time for different surfactant screening coefficients  $\beta$  with  $\phi = 0.05$  in  $D = 3$ . From this figure, we observe that  $N(t)$  initially decays very fast, then slows down, and eventually saturates. The saturation constant is proportional to  $\beta^D$

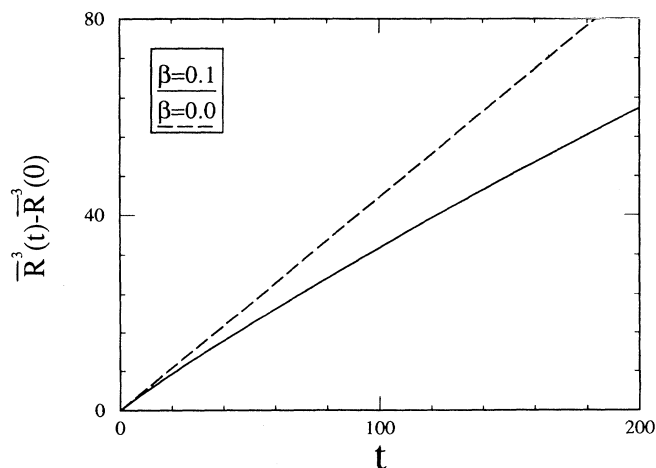


FIG. 6. Comparison of the growth  $\bar{R}^3(t) - \bar{R}^3(0)$  vs  $t^{1/3}$  between  $\beta = 0$ , i.e.,  $\alpha = 0$  (dashed line), and  $\beta = 0.1$ , i.e.,  $\alpha = 2.8 \times 10^{-4}$  (solid line), in  $D = 2$ .

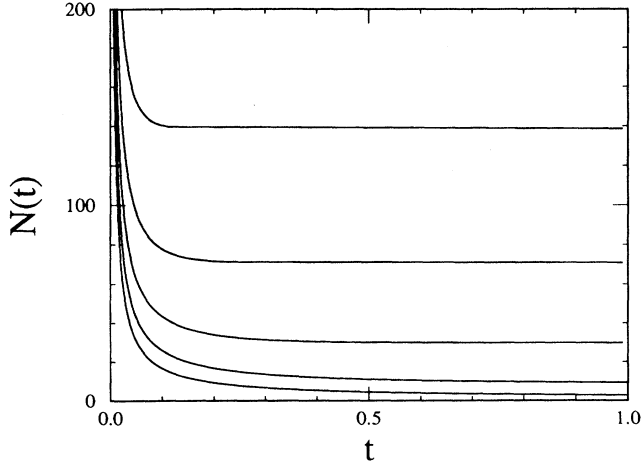


FIG. 7. Decay of the total number of droplets with time in  $D = 3$ . From bottom to top the values of  $\beta$  are 1, 2, 3, 4, and 5 ( $\alpha = 2.2 \times 10^{-3}, 4.4 \times 10^{-3}, 6.6 \times 10^{-3}, 8.8 \times 10^{-3}$ , and  $1.1 \times 10^{-2}$ ), respectively, in  $D = 3$ .

as expected due to the fact that as the average surfactant concentration increases, more interfaces are needed to locate them. Note that if  $\beta = 0$ ,  $N(t)$  will decay as  $t^{-D/3}$ .

The evolution of the average radius and number of droplets as a function of time can also be observed from the evolution of the droplet size distribution function. Substituting Eq. (18) into (17) gives us the distribution function for the droplet size:

$$f(R, t) \propto \frac{1}{u^{D+1}(t)} g\left(\frac{R}{u(t)}\right), \quad (32)$$

which is plotted in Fig. 8 for  $\beta = 1$  with  $\phi = 0.05$  in  $D = 3$ . The area under  $f(R, t)$  in Fig. 8 is proportional to the total number of the droplets. At early times,

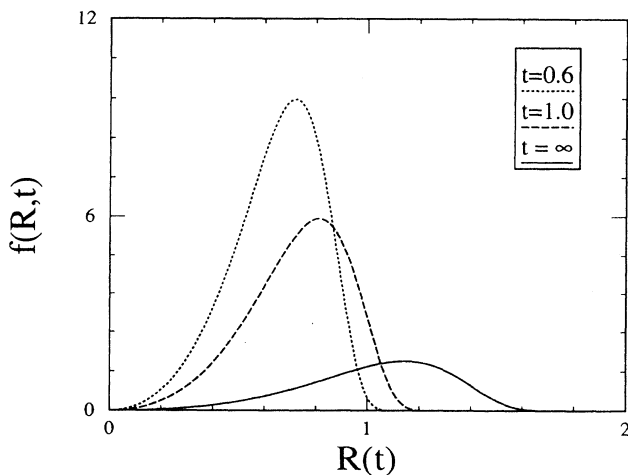


FIG. 8. The evolution of the distribution function  $f(R, t)$  of droplet size  $R$  for different times in  $D = 3$ ,  $\phi = 0.05$ , and  $\beta = 1$ .

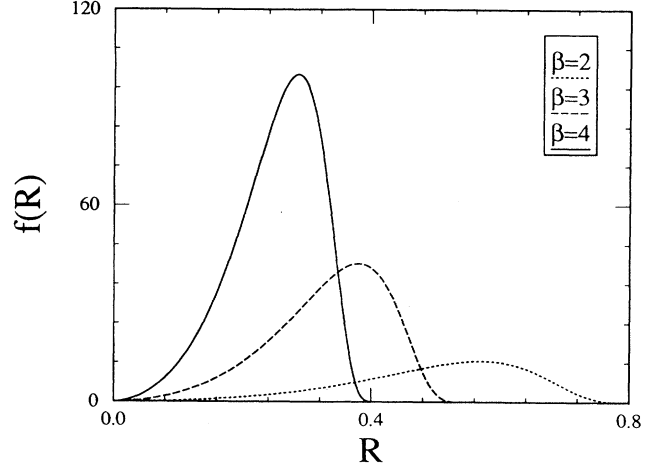


FIG. 9. The equilibrium ( $t \rightarrow \infty$ ) distribution function  $f(R)$  of droplet size  $R$  for  $\phi = 0.05$ , but different  $\beta$  in  $D = 2$ .

this area decays, whereas the maximum droplet radius and the average droplet radius increase. At very late times, the area, the maximum radius, and the average radius no longer vary with time, and the system reaches equilibrium. In contrast, in the absence of surfactants, the area under  $f(R, t)$  becomes vanishingly small when time approaches infinity [11]. In Fig. 9, we compare the equilibrium behavior (i.e., as  $t \rightarrow \infty$ ) of the distribution functions for different values of  $\beta$  in two dimensions. We observe, as expected, that as the amount of surfactants is increased, the position of the maximum of  $f(R)$  decreases, whereas its maximum value increases. Similar behavior is also observed in three dimensions.

#### IV. CONCLUSION

In conclusion, we have applied the theory of Ostwald ripening [11] to systems consisting of two immiscible components and a small amount of surfactants by introducing an effective time-dependent surface tension. We predict that any time-dependent surface-tension problem can be mapped onto a constant-surface-tension case, and that the time dependence of the surface tension has no effect on the scaled distribution function, even though the growth no longer obeys a  $t^{1/3}$  law. Of course, our theory is only valid for systems in which the concentration field reaches a steady state and the droplets have spherical shapes with sharp interfaces; some cases we studied in this article might not satisfy these conditions.

Although our theory is applicable in small volume fraction ( $\phi \leq 6\%$  in  $D = 3$  or  $8.5\%$  in  $D = 2$ ) systems [11], its results, we believe, are not essentially different from systems with higher volume fraction. Nevertheless, we do not know of any experimental results on the effects of surfactants on the dynamics of phase separation in the literature. Thus, we have not been able to compare our predictions with experiments. We think that the present theory and the previous numerical simulations [21, 22]

need to be examined by experiments. We propose that a mixture of two incompatible homopolymers and diblock copolymers would be a good candidate for such experiments.

#### ACKNOWLEDGMENTS

We would like to thank Professor Martin Grant, Professor Martin J. Zuckermann, and Professor Hong Guo

for their helpful discussions, constructive criticism, and encouragement. We would also like to thank Dr. Ken Elder for useful discussions and constructive criticism. This work was supported by the Natural Sciences and Engineering Research Council of Canada and le Fonds pour la Formation de Chercheurs et l'Aide à la Recherche de la Province de Québec. J.H.Y. acknowledges support from the Alexander McFee Foundation and M.L., from the Dow Hickson Foundation.

- 
- [1] I. M. Lifshitz and V. V. Slyozov, *J. Phys. Chem. Solids* **19**, 35 (1961).
- [2] C. Wagner, *Z. Electrochem.* **65**, 581 (1961).
- [3] J. D. Gunton, M. San Miguel, and P. S. Sahni, in *Phase Transitions and Critical Phenomena*, edited by C. Domb and J. L. Lebowitz (Academic, London, 1983), Vol. 8.
- [4] J. A. Marqusee and J. Ross, *J. Chem. Phys.* **80**, 536 (1984).
- [5] J. A. Marqusee, *J. Chem. Phys.* **81**, 976 (1984).
- [6] M. Tokuyama and K. Kawasaki, *Physica A* **123**, 386 (1984); K. Kawasaki and Y. Enomoto, *ibid.* **134**, 323 (1986); **135**, 426 (1986); Y. Enomoto, M. Tokuyama, and K. Kawasaki, *Acta Metall.* **34**, 2119 (1986).
- [7] P. W. Voorhees and M. E. Glicksman, *Acta Metall.* **32**, 2001 (1984); **32**, 2013 (1984); P. W. Voorhees, *J. Stat. Phys.* **38**, 231 (1985); P. P. Ewald, *Ann. Phys. (N.Y.)* **64**, 253 (1982).
- [8] M. Marder, *Phys. Rev. Lett.* **55**, 2953 (1985); *Phys. Rev. A* **36**, 858 (1987).
- [9] Q. Zheng and J.D. Gunton, *Phys. Rev. A* **39**, 4848 (1989).
- [10] A. J. Ardell, *Phys. Rev. B* **41**, 2554 (1990); *Acta Metall.* **20**, 61 (1972).
- [11] J. H. Yao, K.R. Elder, H. Guo, and M. Grant, *Phys. Rev. B* **45**, 8173 (1992); *Phys. Rev. B* (to be published); J. H. Yao, Ph.D. thesis, McGill University, Canada, 1992 (unpublished).
- [12] *Physics of Amphiphilic Layers*, edited by J. Meunier, D. Langevin, and N. Boccarda (Springer-Verlag, Berlin 1987), Part VI, and references therein.
- [13] M. Kotlarchyk, S.-H. Chen, J. S. Huang, and M. W. Kim, *Phys. Rev. B* **29**, 2054 (1984); *Phys. Rev. Lett.* **53**, 941 (1984).
- [14] S. A. Safran and L. A. Turkevick, *Phys. Rev. Lett.* **50**, 1930 (1983); S. T. Milner, S. A. Safran, D. Andelman, M. E. Cates, and D. Roux, *J. Phys. (Paris)* **49**, 1065 (1988).
- [15] G. Gompper and M. Schick, *Phys. Rev. Lett.* **62**, 1647 (1989); *Phys. Rev. A* **42**, 2137 (1990); *Phys. Rev. B* **41**, 9148 (1990).
- [16] J. Matsen and D. E. Sullivan, *Phys. Rev. A* **41**, 2021 (1990).
- [17] M. Laradji, H. Guo, M. Grant, and M. J. Zuckermann, *Phys. Rev. A* **44**, 8184 (1991).
- [18] K. Chen, C. Jayaprakash, R. Pandit, and W. Wenzel, *Phys. Rev. Lett.* **65**, 2736 (1990).
- [19] Z.-G. Wang and S. A. Safran, *J. Phys. (Paris)* **51**, 185 (1990); *J. Chem. Phys.* **94**, 679 (1991).
- [20] R. Holyst and M. Schick, *J. Chem. Phys.* **96**, 7728 (1992).
- [21] M. Laradji, H. Guo, M. Grant, and M. J. Zuckermann, *J. Phys. A* **24**, L629 (1991); *J. Phys. Condens. Matter* **4**, 6715 (1992).
- [22] K. Kawasaki and T. Kawakatsu, *Physica* **164**, 549 (1990); T. Kawakatsu and K. Kawasaki, *ibid.* **167**, 690 (1990).
- [23] The separation factor  $\lambda$  and the coarsening rate  $K(\phi)$  have been discussed in Ref. [11].
- [24] There may be some relationship between the behavior studied analytically here and the numerical work by M. Bahiana and Y. Oono, *Phys. Rev. A* **41**, 6763 (1990), and that by F. Liu and N. Goldefeld, *Phys. Rev. A* **39**, 4805 (1989).
- [25] In Fig. 5, we have rescaled the numerical data of Laradji *et al.* by introducing two parameters  $A$  and  $B$  according to  $\bar{R}(t)/t^{1/3} = Ah(B\beta^3 t)$  due to the fact that they used different time and length scales from those used in the present paper.